

# Exergo-Ecological Assessment of Waste to Energy Plants Supported by Solar Energy

## **Authors:**

Barbara Mendecka, Lidia Lombardi, Paweł Gładysz, Wojciech Stanek

*Date Submitted:* 2020-06-23

*Keywords:* thermoecological cost, WtE plant, exergy analysis, solar energy

## **Abstract:**

Hybridization of Waste to Energy (WtE) plants with solar facilities can take competing energy technologies and make them complementary. However, realizing the benefits of the solar integration requires careful consideration of its efficiency. To analyse such systems from the point of view of resource efficiency, the pure energy analysis is not sufficient since the quality of particular energy carriers is not evaluated. This work applies the exergo-ecological analysis using the concepts of thermoecological cost (TEC) and exergy cost for the performance evaluation of an integrated Solar-Waste to Energy plant scheme, where solar energy is used for steam superheating. Different plant layouts, considering several design steam parameters as well as different solar system configurations, in terms of area of heliostats and size of the thermal storage tank, were studied. The results for the solar integrated plant scheme were compared with the scenarios where superheating is performed fully by a non-renewable energy source. The presented results of exergy cost analysis indicate that the most favorable system is the one supported by non-renewable energy. Such an analysis does not consider the advantage of the use of renewable energy sources. By extending the system boundary to the level of natural resource and applying the thermoecological cost analysis, an opposite result was obtained.

*Record Type:* Published Article

*Submitted To:* LAPSE (Living Archive for Process Systems Engineering)

*Citation (overall record, always the latest version):*

LAPSE:2020.0730

*Citation (this specific file, latest version):*

LAPSE:2020.0730-1

*Citation (this specific file, this version):*


LAPSE:2020.0730-1v1

*DOI of Published Version:* <https://doi.org/10.3390/en11040773>

*License:* Creative Commons Attribution 4.0 International (CC BY 4.0)

Article

# Exergo-Ecological Assessment of Waste to Energy Plants Supported by Solar Energy

Barbara Mendecka <sup>1</sup> , Lidia Lombardi <sup>2,\*</sup>, Paweł Gładysz <sup>3</sup> and Wojciech Stanek <sup>4</sup>

<sup>1</sup> Department of Industrial Engineering, University of Florence, 50121 Florence, Italy; barbara.mendecka@unifi.it

<sup>2</sup> Department of Engineering, Niccolò Cusano University of Rome, 00166 Rome, Italy

<sup>3</sup> Faculty of Energy and Fuels, AGH University of Science and Technology, 30059 Krakow, Poland; pawel.gladysz@agh.edu.pl

<sup>4</sup> Institute of Thermal Technology, Silesian University of Technology, 44100 Gliwice, Poland; wojciech.stanek@polsl.pl

\* Correspondence: lidia.lombardi@unicusano.it; Tel.: +39-366-638-1000

Received: 28 February 2018; Accepted: 27 March 2018; Published: 28 March 2018



**Abstract:** Hybridization of Waste to Energy (WtE) plants with solar facilities can take competing energy technologies and make them complementary. However, realizing the benefits of the solar integration requires careful consideration of its efficiency. To analyse such systems from the point of view of resource efficiency, the pure energy analysis is not sufficient since the quality of particular energy carriers is not evaluated. This work applies the exergo-ecological analysis using the concepts of thermoecological cost (TEC) and exergy cost for the performance evaluation of an integrated Solar-Waste to Energy plant scheme, where solar energy is used for steam superheating. Different plant layouts, considering several design steam parameters as well as different solar system configurations, in terms of area of heliostats and size of the thermal storage tank, were studied. The results for the solar integrated plant scheme were compared with the scenarios where superheating is performed fully by a non-renewable energy source. The presented results of exergy cost analysis indicate that the most favorable system is the one supported by non-renewable energy. Such an analysis does not consider the advantage of the use of renewable energy sources. By extending the system boundary to the level of natural resource and applying the thermoecological cost analysis, an opposite result was obtained.

**Keywords:** solar energy; WtE plant; exergy analysis; thermoecological cost

## 1. Introduction

The strategy of the European Union (EU) for waste prevention and management is based on the following hierarchy: prevention; preparing for re-use; recycling; other recovery, e.g., energy recovery; and disposal [1]. Thus, for those streams of waste, for which the material recovery is not effectively applicable, the energy recovery is the path to be followed, while landfilling must be residual and devoted to pre-treated wastes. Recently, the European Commission [2] communicated that the role of waste-to-energy (WtE) processes (including both thermal and biological processes) can assist in the transition to a circular economy, strengthening the concept that the EU waste hierarchy is the guiding principle and that choices made toward the WtE must not prevent higher levels of prevention, reuse and recycling.

Residual non-recyclable wastes downstream prevention, reuse and recycling still have interesting energy content [3]. For example residual municipal solid waste (MSW) in EU has a low heating value (LHV) of about 10.3 GJ/Mg [4], with about 50% share of renewable carbon content [5].

Gasification of MSW has been proposed as energy conversion method. It was shown that the process could be enhanced when MSW is reduced to small particle sizes [6]. However, among others possible thermal treatments for energy recovery from waste, nowadays, combustion processes—in the following simply named WtE—are the most commonly widespread and applied for different types of waste, including MSW [7].

The WtE power plants have a strong potential in the perspective of fossil energy displacement [8]. However, the efficiency of the existing WtE plants is limited due to high-temperature corrosion problem [9,10]. The typical WtE plant operates at a steam pressure of 40 bars and temperature of 400 °C [11]. Taking into consideration relatively high parasitic consumption of the power plant and such steam parameters, the net efficiency of the WtE plant is typically in the range 22–25%, while values up to a maximum of 30% can be reached only in large installations [12].

Further improvements of energy efficiency are possible by the introduction of the external superheater. Eliminating the superheater from the WTE boiler increases reliability and decreases costs [13]. Such a solution allows the superheated steam temperature to be raised, without the above-mentioned corrosion risk. External superheating can be performed with the use of solar energy. Employing solar energy in electricity generation creates economic opportunities and environmental improvements [14]. The potential advantages of this arrangement are presented in the previous study of authors [15]. In that work, thermodynamic and economic performances of the integrated system of a 50 MW thermal power input WtE plant coupled with a solar tower were investigated. It was found that the improvement up to 4.5% of net energy efficiency can be obtained when the external superheating is introduced.

However, by comparing the thermal efficiency and exergetic efficiency of the systems, it is often concluded that thermal efficiency is not sufficient to choose the desired system. Direct exergy analysis enables to highlight the main components having high thermodynamic inefficiencies [16]. Moreover, it takes into account the quality difference between work and heat and/or cold at different temperatures [17]. Using the exergetic efficiency as the optimization criterion provide a direction for improving the overall efficiency of a power plant [18].

As far as performance evaluation of high-temperature solar energy applications is concerned, numerous studies on exergetic analysis can be found in the literature. As an example, Toro et al. [19] evaluated the solar concentrated power plant with the central receiver from exergy and thermo-economic point of view. Regarding hybrid fossil fuel plants integrated with solar power, the conventional exergetic analysis has been applied to evaluate the exergy destructions of the components in the solar tower aided coal power plant [20,21]. In another example, optimum choice of method of integration of the solar subsystem with the gas combined cycle was studied [22,23].

Mathkor et al. [24] and Bellos et al. [25] have demonstrated the importance of exergetic analysis, when evaluating the performance of the solar-driven Organic Rankine Cycle tri-generation system. Calise et al. have applied exergy analysis for the performance evaluation of polygeneration system integrating solar and other renewable sources [26,27].

In general, the studies on exergy analysis in solar driven energy systems conclude that the highest exergy destructions occur in the solar subsystem. Thus, considerable efforts should be focused on reducing the exergy loss in the central receiver component, which mainly depends on the operating temperature. Another finding is that the second law efficiency of the solar integrated power plant is lower than the plant without solar contribution.

Nevertheless, it should be underlined that the traditional exergy analysis does not distinguish the irreversibilities caused by the components supplied by renewable and non-renewable energy. A reduction of the internal irreversibilities within a given system may not always be accompanied by a reduction of its primary energy-resources requirements. It was previously found [28] that any solution which combines both renewable and non-renewable resources should be verified in an extended boundary perspective using cumulative or life cycle analysis. These requirements are fulfilled by the thermoecological cost (TEC) analysis.

Thermoeological cost (TEC) has been defined by Szargut [29,30] as the cumulative consumption of non-renewable exergy of natural resources burdening fabrication of any useful product with the additional inclusion of the consumption resulting from the necessity of compensating the environmental losses caused by the rejection of harmful waste substances to the environment. The Szargut's method (in contrast to other methods of ecological assessment), can bring all environmental impacts into one measure which is the exergy of the consumed natural, non-renewable resources.

The TEC concept has been applied in numerous studies concerning the evaluation of renewable or non-conventional energy systems. As an example, it was applied to evaluate biofuel conversion processes [31,32], to assess environmental impacts of electricity production by micro wind turbines with vertical axis [33]. The potential of this approach in the case of multigeneration systems is efficiently demonstrated in [34,35].

This work applies the exergo-ecological analysis using the concepts of thermoeological cost and exergy cost for integrated solar—Waste to Energy plant scheme. More specifically, different plant layouts are simulated varying the superheated steam parameters (pressure and temperature). Such analysis is an original contribution to the existing literature. In this work, we assume three different steam parameters values (couples of pressure and temperature), for the integrated system, representative of the previously investigated ranges [15], which are: 51 bar and 440 °C; 60 bar and 480 °C and 70 bar and 520 °C. The upper limit for the superheated steam temperature is 520 °C. It is imposed by the maximum temperature allowable for the molten salts, which cannot be higher than 565 °C. The lower superheated steam pressure is 51 bar. This limit is imposed by the minimum temperature imposed for the salts, since they solidify at 290 °C, assuming a temperature difference between the temperature of the salts and the saturated steam one of 25 °C. The solar field resulting from the three different couples of steam parameters was analyzed using solar multiples (SM) in a range from 1.5 to 2.5 (intervals with 0.5 SM steps). Then thermal storage capacities representing a full load heat source for superheater between 6 h and 14 h (with 4 h step) were considered. The combination of the three different receiver concepts, options for steam parameters and thermal storage capacities led to 27 layouts that are analyzed in detail. Results of the TEC analysis are compared with those obtained by the classic exergy analysis approach. The hybrid system is also compared with the case where the superheating is entirely performed by the external fossil fuel based system.

The remainder of the article is arranged as follows: Section 2 describes the layout of each plant configuration introducing the main design data and assumptions and the adopted methodology; in Section 3, the exergy analysis is performed; in Section 4, the exergy and thermoeological cost analyses are applied, and the results are finally presented and discussed.

## 2. Materials and Methods

### 2.1. Modeling Approach

In studied cases, the resources comprise dominantly wastes and the locally consumed renewables (solar radiation) and non-renewables (natural gas). Firstly, direct exergy analysis is applied to evaluate the exergy cost of electricity as well as sources of internal plant irreversibility and within a local boundary system. Secondly, by considering the origin of the resources supplied to the system, the analysis is performed within an extended control volume reaching the level of extracting natural resources from the nature. Such an approach is recommended for evaluation of the hybrid energy conversion systems in terms of their sustainability.

The design and off-design modeling of the system was done in the EBSILON Professional version 13.0 and Matlab R2013b software. Initially, a reference concept of the WtE plant without external superheater was modeled, to determine the system net power output and overall system efficiency. In the stand-alone case, the WtE net output power is 10.7 MW, and the efficiency is equal to 21.65% [15]. Thereafter, a system with external superheater incorporating a solar thermal input was modeled,

and the effects of the solar thermal input on the overall energy and exergy system performance were investigated.

Off-design performances of the considered plant layouts were evaluated by means of a typical year of operation and off-design changes in thermodynamic performances of the power plant components. The model considers a random availability of solar source, which is important when considering the generation from renewable sources [36]. The WtE plant part was maintained at the design parameters. The charge and discharge of the molten salt storage tanks and backup gas boiler operation were included and accounted for. A control system was added in the CSP part. The control objective is to supply superheated steam at the demanded temperature and pressure, minimizing auxiliary energy (gas) consumption. It assumed that the gas boiler operates only when the hot storage tank level was below 10%, and there was no (or not enough) solar power from the solar receiver available at the given moment. Additionally, when the hot storage tank level was above 90%, the additional control strategy was put in place not to allow the hot storage tank level to go above maximal capacity. In this situation, the part of solar energy available at the receiver was dumped, e.g., by means of heliostat defocusing.

## 2.2. Description and Characteristic of the System

Figures 1 and 2 show a schematic representation of the hybrid WtE plant studied in this paper. The studied concept assumes that the same amount of waste of the standalone WtE case is fed to the boiler grid furnace and the thermal energy generated by the waste combustion is used to pre-heat the feeding water and to produce saturated steam at the assumed pressure condition, by means of economizer and evaporator. Saturated steam is superheated in the external heat exchanger.

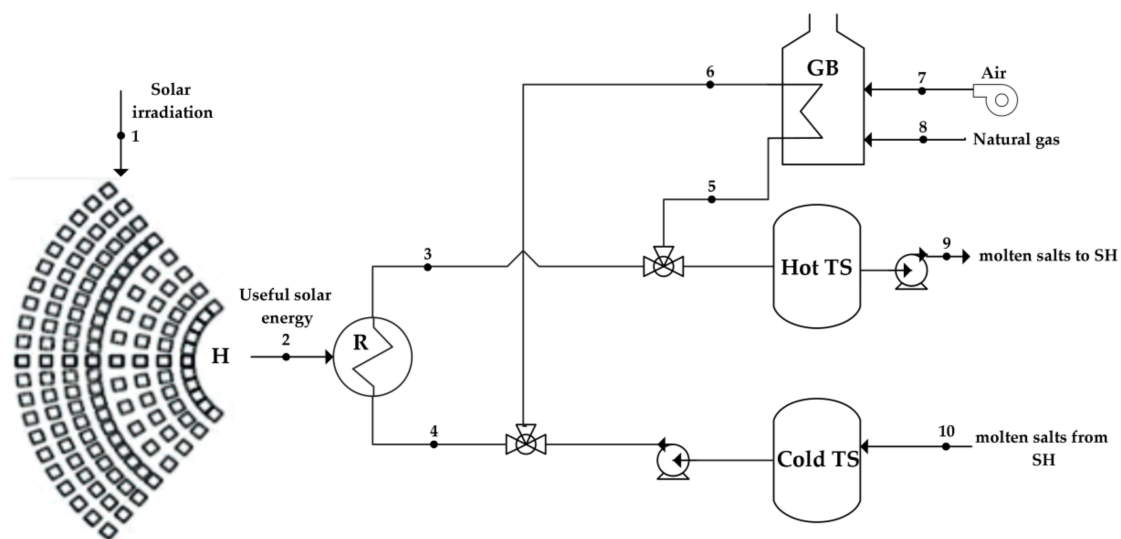


**Figure 1.** Structure of solar system with heliostats and solar tower: H—heliostats, R—receiver, GB—backup gas boiler, Hot TS—hots storage tank, Cold TS—cold storage tank, SH—superheater.

Table 1 presents the performance data for the analyzed cases. Cases 1–27 concern the hybrid solar—WtE plant schemes. Cases 1\*–3\* concern the schemes where the superheating is realized fully by the gas boiler. The more detailed data of the presented systems are presented in Table S1 of the Supplementary Material. The boiler grid furnace is fueled by municipal solid wastes (MSW), with composition reported in [15] and in Table 2, with an LHV equal to  $10.4 \text{ GJ Mg}^{-1}$  (calculated on the chemical composition basis). Usable products of this cycle comprise electricity (net power output).

**Table 1.** Performance outputs and size parameters for analyzed WtE + CSP cases.

Case No.	Steam Parameters	Solar Multiple/Time of Storage	Superheating Power	Storage Tank Size	Heliostat Aperture	Net Electricity Output
	bar/°C	-/h	MW	m <sup>3</sup>	m <sup>2</sup>	MWh year <sup>-1</sup>
1	51.0/440	1.5/6	9.8	462	59,640	123,973
2		1.5/10	9.8	713	59,640	123,973
3		1.5/14	9.8	998	59,640	123,974
4		2.0/6	9.8	571	79,440	123,998
5		2.0/10	9.8	951	79,440	124,007
6		2.0/14	9.8	1331	79,440	124,008
7		2.5/6	9.8	713	99,240	124,013
8		2.5/10	9.8	1189	99,240	124,026
9		2.5/14	9.8	1664	99,240	124,030
10	60.0/480	1.5/6	11.7	510	70,920	133,993
11		1.5/10	11.7	882	70,920	133,994
12		1.5/14	11.7	1235	70,920	133,994
13		2.0/6	11.7	705	94,560	134,022
14		2.0/10	11.7	1176	94,560	134,033
15		2.0/14	11.7	1646	94,560	134,035
16		2.5/6	11.7	882	118,200	134,039
17		2.5/10	11.7	1470	118,200	134,057
18		2.5/14	11.7	2058	118,200	134,062
19	70.0/520	1.5/6	13.6	619	83,040	144,581
20		1.5/10	13.6	1073	83,040	144,582
21		1.5/14	13.6	1502	83,040	144,582
22		2.0/6	13.6	858	110,640	144,616
23		2.0/10	13.6	1430	110,640	144,628
24		2.0/14	13.6	2002	110,640	144,630
25		2.5/6	13.6	1073	138,360	144,636
26		2.5/10	13.6	1788	138,360	144,654
27		2.5/14	13.6	2503	138,360	144,662
1*	51.0/440	-	9.8	-	-	127,973
2*	60.0/480	-	11.7	-	-	138,504
3*	70.0/520	-	13.6	-	-	149,664

**Table 2.** Specific exergy of fuels employed in the analysis.

	Chemical Composition	LHV	$\beta$	Specific Exergy	$ex_{F,i}$
		kJ kg <sup>-1</sup>	-	kJ kg <sup>-1</sup>	kJ kg <sup>-1</sup>
Natural gas [volumetric analysis]	CH <sub>4</sub> : 96.0; C <sub>2</sub> H <sub>6</sub> : 1.3; C <sub>3</sub> H <sub>8</sub> : 0.2; N <sub>2</sub> : 2.5	47,941	1.036	$ex_{F,8} = \beta \times LHV$	49,686
MSW [ultimate analysis]	C: 27.59; H: 4.23 O: 17.39; S: 0.04; N: 0.67; Cl: 0.26; F: 0.004; Ash: 16.46; H <sub>2</sub> O: 33.37	10,411	1.099	$ex_{F,11} = \beta \times (LHV + h_{H_2O} \times [H_2O]) + ex_{H_2O} \times [H_2O] + 9683 \times [S] + ex_{ash} \times [Ashes]$	11,880

In the schemes with the solar cycle, molten salts mixture is considered as the heat transfer fluid. The solar field is composed of heliostats, which reflect and concentrate solar radiation on a receiver located on the upper part of a solar tower. Molten salts are pumped from a cold storage tank through the receiver, where they are heated, and then stored in the hot storage tank. Hot salts are pumped to an external heat exchanger where the steam is superheated to the design temperature, and the exiting salts are returned to the cold storage tank where they are stored. The superheater can be supplied by two different energy sources (solar and gas), which can be combined or used independently, depending on the current conditions. The operation mode can be re-configured manipulating open/close valves and pumps to allow the selection of the components for energy supply. When there is not enough hot molten salt in the hot storage tank (the level of the tank is below 10%), the backup system is started to provide the necessary heat flux for the superheater. The backup system is fueled by natural gas with composition reported in [15] and presented in Table 2, with an LHV equal to 47.9 GJ Mg<sup>-1</sup>.

Superheated steam feeds to the high-pressure steam turbine, and then through medium-pressure and low-pressure parts to the air-cooled condenser. Condensate from the condenser is supplied to the boiler through the one-stage regenerative heat exchanger and deaerator.

The heliostat field was modeled assuming the hypothetical site in the southern part of Italy (13.1° E; 38.2° N), as representative of high solar irradiance. The design point for solar field is solar noon on 21 June. In order to conduct a daily and an annual performance calculation on an hourly basis, local hourly values of direct normal irradiation, wind speed and other weather conditions for the whole year were obtained from the typical meteorological year (TMY) of Meteonorm database [13].

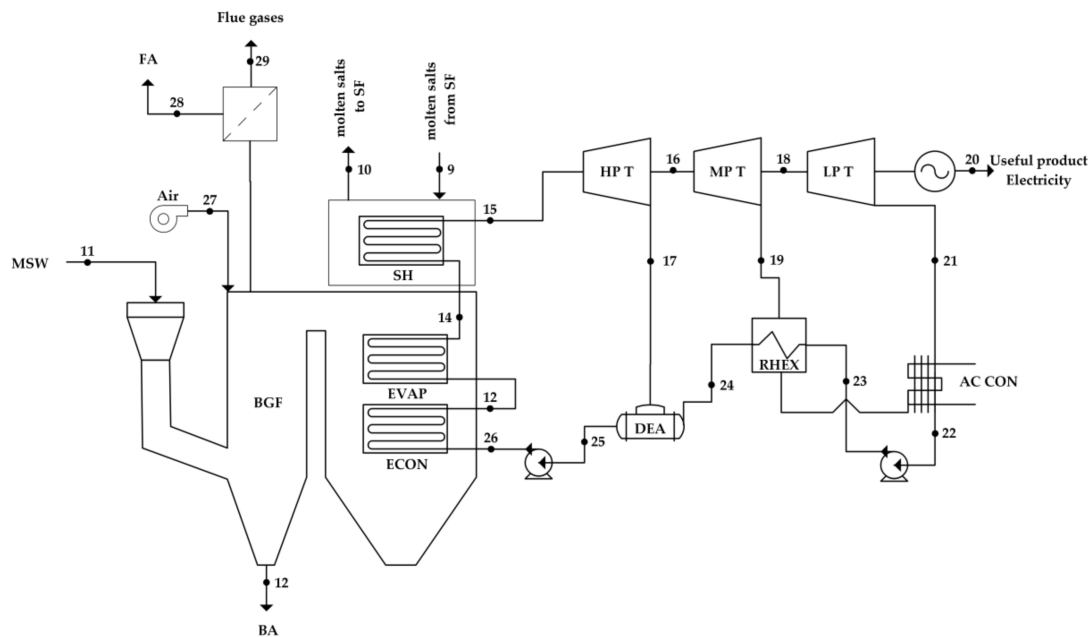


**Figure 2.** Structure of WtE Rankine cycle: MSW—municipal solid wastes, BGF—boiler furnace, ECON—economizer, EVAP—evaporator, SH—superheater, HP T—high pressure turbine, MP T—Medium pressure turbine, LP T—low pressure turbine, AC CON—air-cooled condenser, RHEX, regenerative heat exchanger, DEA—deaerator, FA—fly ashes, BA—bottom ashes.

### 2.3. Thermo-economic and Thermoecological Analysis

The exergy analysis of the entire system is carried out by combining the analysis for each subsystem, which is based on the exergy balance for a control volume. The study is performed assuming transient conditions and the results are presented for the average yearly operation. Moreover, the following assumptions are made: pressure drops and heat losses in pipelines are neglected, and kinetic and potential exergy are ignored.

In general term, exergy balance represents the renewable and non-renewable inputs ( $F$ ), products ( $P$ ), external losses ( $L$ ) and internal exergy destructions ( $D$ ):

$$\sum Ex_F = \sum Ex_P + \sum Ex_L + \sum Ex_D \quad (1)$$

The psychical exergy of each state point is considered as:

$$Ex_i = m_i \times ((h_i - h_0) - T_0(s_i - s_0)) \quad (2)$$

where  $m_i$  is the mass of substance under consideration;  $h_i$ ,  $s_i$  are, respectively, the enthalpy and entropy of considered matter, and  $h_0$ ,  $s_0$  are the enthalpy and entropy of this matter in an equilibrium state with

environment of temperature  $T_0$ . The structure of electricity production is evaluated by the contribution of the exergy of particular input to the total input exergy, calculated as follows:

$$\varepsilon_i = \frac{Ex_{F,i}}{\sum Ex_{F,i}} \quad (3)$$

Calculations of the specific chemical exergy for the input fuels ( $ex_{F,8}$ ,  $ex_{F,11}$ ) require the knowledge of reference exergies of the elements and the chemical composition of the fuels. Table 2 shows the chemical compositions of the fuels, adapted from [15], basing on the ultimate analysis for MSW and volumetric analysis for the natural gas. The values of the standard molar specific enthalpy of devaluation and the standard molar specific chemical exergy of the components of the reactants and the products are taken from [37]. The specific exergy values of the fuels are calculated using methodology presented in [29,38]. The exergy input of the fuels (here, municipal solid wastes and natural gas) is calculated using Equation (4):

$$Ex_{F,i} = m_{F,i} \times ex_{F,i} \quad (4)$$

The total exergy received by the heliostat subsystem is proportional to the total aperture area of  $A_{heliostat}$  and the specific solar exergy  $ex_{F,1}$  and is given by Equation (5):

$$Ex_{F,1} = A_{heliostat} \times ex_{F,1} \quad (5)$$

The specific exergy of the solar radiation  $ex_{F,1}$  [ $W/m^2$ ] is calculated using the Equation (6) adapted from Petela and Szargut [29,39] and used in similar studies [22,40,41]:

$$ex_{F,1} = e_{F,1} \times \left( 1 - \frac{4}{3} \times \frac{T_0}{T} + \frac{1}{3} \times \left( \frac{T_0}{T} \right)^4 \right) \quad (6)$$

where  $e_{F,1}$  is the solar irradiance reaching the heliostat [ $W/m^2$ ],  $T$  is the absolute temperature of the emitting surface, here assumed constant and equal to 5870 K, and  $T_0$  is the temperature of the environment.

Exergy transferred from the solar source to the heliostat is partially delivered to the central receiver system and the remaining fraction  $Ex_{L,1}$  is lost to the environment. Exergy balance of the heliostat can be written as follows:

$$Ex_{F,1} = Ex_2 + Ex_{L,1} \quad (7)$$

The central receiver absorbs the solar exergy  $Ex_2$ , part of it is lost through the convective, conductive and radiation heat transfer. The remaining part is transferred to the heat transfer fluid. Exergy balance of the receiver is closed by the internal exergy losses  $Ex_{D,2}$ . Exergy absorbed by the molten salts is calculated by Equation (8):

$$Ex_2 = \Delta Ex_{4-3} + Ex_{L,2} + Ex_{D,2} \quad \text{and} \quad \Delta Ex_{4-3} = m_{3-4} \times ((h_4 - h_3) - T_0(s_4 - s_3)) \quad (8)$$

In order to calculate the average values of the efficiencies of the system components, the hourly ( $d\tau = 1$  h) efficiencies are considered. The average exergy efficiency of the heliostat and receiver subsystems over the interval of the operating time, assumed here as a whole year operation ( $\tau_{op} = 8760$  h) is calculated as follows:

$$\bar{\eta}_{Ex, heliostat} = \frac{1}{\tau_{op}} \int_0^{\tau_{op}} \left( \frac{Ex_1}{Ex_2} \right) d\tau \quad \text{and} \quad \bar{\eta}_{Ex, receiver} = \frac{1}{\tau_{op}} \int_0^{\tau_{op}} \left( \frac{Ex_2}{\Delta Ex_{4-3}} \right) d\tau \quad (9)$$



The second law efficiency of heliostat-receiver subsystem for the whole year of operation is given by the Equation (10):

$$\bar{\eta}_{Ex, heliostat-receiver} = \frac{1}{\tau_{op}} \int_0^{\tau_{op}} \left( \frac{m_{3-4} \times ((h_4 - h_3) - T_0(s_4 - s_3))}{Ex_{F,1}} \right) d\tau \quad (10)$$

The annual distribution of the heliostat and receiver efficiencies is presented in Figure 3. In the case of heliostats, the energy and exergy efficiencies are equal to each other due to the fact that losses to the environment are caused by shading, blocking and cosine mechanisms, and no internal irreversibility within the system occurs. The resulting fluxes of useful energy and exergy produced in the heliostat-receiver system are presented in Figure 4.

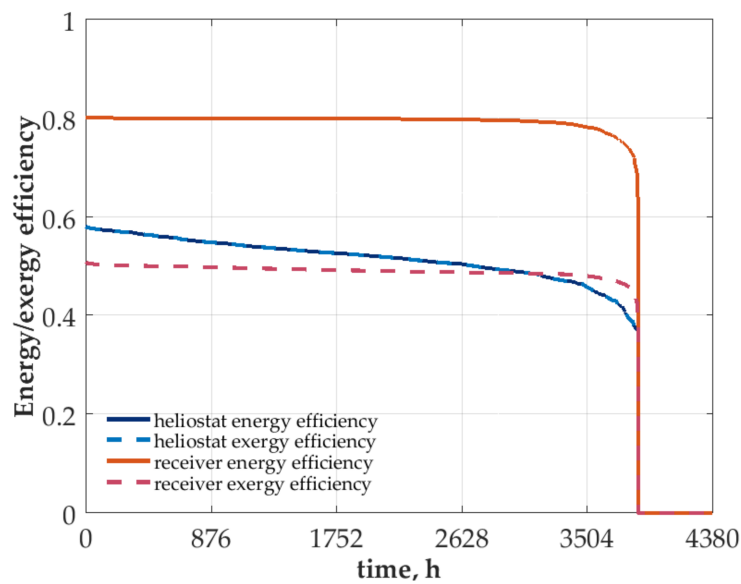


Figure 3. Annual load curve for the heliostat and receiver efficiencies.

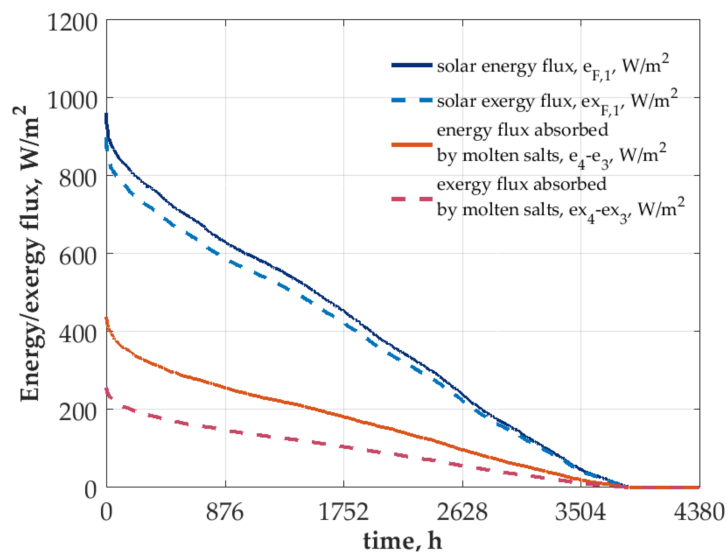


Figure 4. Distribution of the solar radiation energy and exergy during the year.

The accessibility of solar radiation limits the operation of the solar subsystem. Basing on the data presented in Figures 3 and 4 it can be noticed that the total working time of the heliostat-receiver system is constrained to 3860 h/year, which is 44% of the annual operation time.

The required exergy transferred from the molten salts to steam is provided by the heat exchanger. The exergy loss  $Ex_{L14-15}$  is due to the reduction in the quality of thermal energy as it is transferred from a higher to a lower temperature. Exergy balance of the superheater can be written as follows:

$$m_{9-10} \times ((h_{10} - h_9) - T_0(s_{10} - s_9)) = m_{14-15} \times ((h_{15} - h_{14}) - T_0(s_{15} - s_{14})) + Ex_{L14-15} \quad (11)$$

where molten salts flow  $m_{9-10}$  at the desired temperature are provided by solar and gas sources, which can be combined or used independently according to the current solar availability.

Exergy balance for thermal storage system considers charging and discharging state and includes the momentary changes of internal exergy, input, and output flow as well as irreversibility due to contact with the external environment:

$$m_{3-4} \times ((h_4 - h_3) - T_0(s_4 - s_3)) = \frac{dEx_{TES}}{d\tau} + m_{9-10} \times ((h_{10} - h_9) - T_0(s_{10} - s_9)) + Ex_{L,tes} \quad (12)$$

where  $\frac{dEx_{TES}}{d\tau} = \frac{dM_{TES}}{d\tau} \times ((u_{in} - u_{out}) - T_0(s_{in} - s_{out}))$

The average second law efficiency of the thermal storage is given by relation (13):

$$\bar{\eta}_{Ex,tes} = \frac{1}{\tau_{op}} \int_0^{\tau_{op}} \left( \frac{m_{3-4} \times ((h_4 - h_3) - T_0(s_4 - s_3))}{m_{9-10} \times ((h_{10} - h_9) - T_0(s_{10} - s_9))} \right) d\tau \quad (13)$$

Moreover, the second law efficiency of the backup boiler is given by relation (14):

$$\bar{\eta}_{Ex,backup} = \frac{1}{\tau_{op}} \int_0^{\tau_{op}} \left( \frac{m_{5-6} \times ((h_5 - h_6) - T_0(s_5 - s_6))}{m_{F,8} \times ex_{F,8}} \right) d\tau \quad (14)$$

The second law efficiency of MSW furnace producing saturated steam at design pressure is given by Equation (15):

$$\bar{\eta}_{Ex,WtE} = \frac{1}{\tau_{op}} \int_0^{\tau_{op}} \left( \frac{m_{14-26} \times ((h_{14} - h_{26}) - T_0(s_{14} - s_{26}))}{m_{F,11} \times ex_{F,11}} \right) d\tau \quad (15)$$

Bottom steam cycle is considered as the one subsystem thus exergy loss  $Ex_{L26-15}$ , considers irreversibilities occurring in turbine, condenser, deaerator, regenerative heat exchanger and pumps. Simplified exergy balance of bottom steam cycle is given by Equation (16):

$$Ex_{20} = m_{15-26} \times ((h_{15} - h_{26}) - T_0(s_{15} - s_{26})) + \sum Ex_{L15-26} \quad (16)$$

Finally, the second law efficiency of the integrated system is defined by relation (17):

$$\eta_{ex} = \frac{Ex_p}{Ex_{F,11} + Ex_{F,g2} + Ex_{F,1}} \rightarrow c_{ex} = \frac{1}{\eta_{ex}} \quad (17)$$

where  $Ex_p$ —is the system's total net power output,  $Ex_F$  is the exergy provided by the input municipal wastes, the gas backup system and solar exergy input and  $c_{ex}$  is the exergy cost of electricity.

The value of TEC is calculated from the balance of cumulative non-renewable exergy consumption. The total value of TEC burdening the products of the  $j$ -th process results first, from the direct consumption of non-renewable exergy resources supplied to the process.

The balance of TEC of  $j$ -th production branch also includes an additional consumption of resources connected with the waste rejection to the environment  $p_{kj}$ . This additional consumption is linked to the maintenance and operation of abatement installations as well as from the necessity of compensation

of other losses in the environment. Under these assumptions the index of operational TEC can be determined by solving the set of thermo-ecological cost balance equations which general form is presented by Equation (18). The detailed description of the balance method with relevant examples is given in references [29,30,42]:

$$\rho_j + \sum_i (f_{ij} - a_{ij}) \rho_i = \sum_s b_{sj} + \sum_k p_{kj} \zeta_k \quad (18)$$

where:  $a_{ij}$  is a coefficient of the consumption of the  $i$ -th product per unit of the  $j$ -th major product, e.g., in kg/kg or kg/MJ,  $f_{ij}$  is a coefficient of the consumption and by production of the  $i$ -th product per unit of the  $j$ -th major product, e.g., in kg/kg or kg/MJ,  $b_{sj}$  is an exergy of the  $s$ -th non-renewable natural resource immediately consumed in the process under consideration per unit of the  $j$ -th product, MJ/kg,  $\rho_i$  is a specific thermo-ecological cost of the  $i$ -th product, e.g., in MJ/kg,  $p_{kj}$  is an amount of  $k$ -th harmful substance from  $j$ -th process, kg and  $\zeta_k$  is a thermo-ecological cost of  $k$ -th harmful substance, MJ/kg.

The general form of the equation to calculate the thermo-ecological cost in the whole life cycle has been formulated by Szargut [29]. This function, comprises the construction, operational and end-of-life phases, and it is expressed by the following Equation (19):

$$\rho_j^{LCA} = \tau_{op} \left( \sum_i \dot{G}_i \rho_i + \sum_k \dot{P}_k \zeta_k - \sum_u \dot{G}_u \rho_u s_{iu} \right) + \frac{1}{\tau_j} \left( \sum_l G_l \rho_l (1 - u_l) + \sum_r G_r \rho_r \right) \quad (19)$$

where  $\tau_j$  is a nominal lifetime of the  $j$ -th machine, device, installation or building, in years,  $\tau_{op}$  refers to an average time of exploitation of the  $j$ -th considered machine, devices, installation or building, other words annual operation time with nominal capacity, h/year,  $\dot{G}_i$  and  $\dot{G}_u$  are a nominal stream of  $i$ -th product and  $u$ -th by-product manufactured simultaneously in  $j$ -th production process, kg/h,  $s_{iu}$  is a replacement index of by-product  $u$  by main product  $i$ ,  $\dot{P}_k$  is a nominal stream of  $k$ -th waste product released to the environment from the  $j$ -th production process, kg/h,  $G_l$  and  $G_r$  are amounts of  $l$ -th product used for the construction and amount of  $r$ -th product used for the maintenance of  $j$ -th considered machine, device, installation or building, kg and  $u_l$  is an expected recovery rates of the  $l$ -th material after the end of operation phase of  $j$ -th considered machine, device, installation or building, kg/kg.

### 3. Results Exergy and Thermo-Ecological Analysis

The performance parameters defined in Section 2 are calculated here for all the 27 system configurations assuming average annual operation. Results are compared with the ones obtained for the WtE plant combined with fossil fuel-based superheater. In addition, a sensitivity analysis was performed to identify the major parameters affecting the exergy cost and TEC of electricity production.

Figure 5 presents the structure of electricity production in the analyzed cases. As can be observed, the major contribution to the electricity production is the input MSW with a share varying from 79% up to 89%. The remaining share, which is composed of solar and natural gas inputs, increases for cases with higher steam temperature and pressure.

Results of the exergy cost analysis at the lower aggregation level for the two marginal cases are presented in Table 3. Only results for relevant components are reported, considering the average yearly operating conditions.

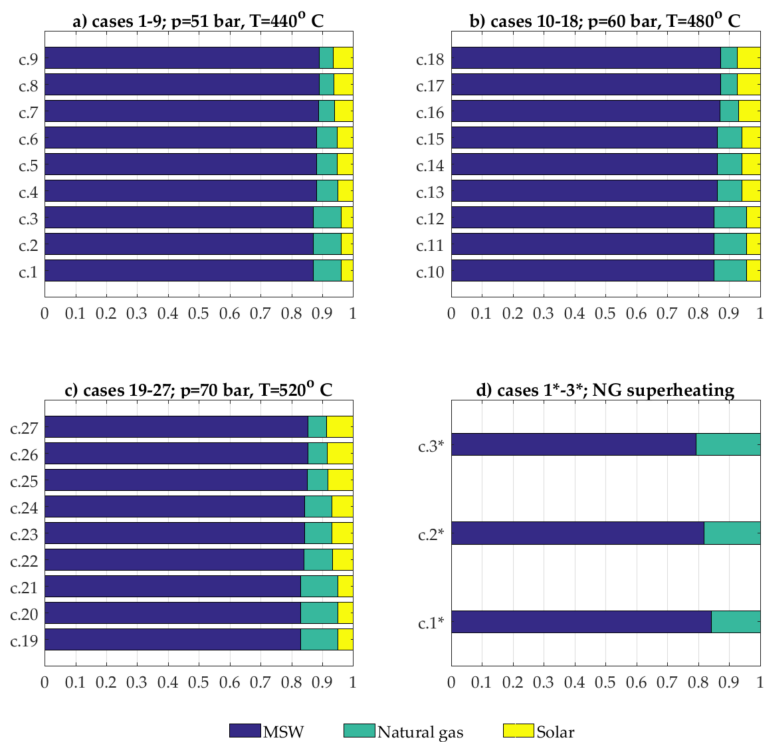


Figure 5. Structure of the electricity production in the analyzed cases (a–d).

Table 3. Exemplary results of the exergy analysis for the solar subsystem (case 1 and 27).

Subsystem	Exergy Received		Exergy Loss		Second Law Efficiency		Exergy Cost	
	MW		MW		%		MW/MW	
Case No.	Case 1	Case 27	Case 1	Case 27	Case 1	Case 27	Case 1	Case 27
Heliostat	9.945	23.059	4.840	11.1872	51.33	51.49	1.948	1.942
Receiver	5.105	11.872	2.595	6.0391	49.17	49.13	2.034	2.035
Tank	2.511	5.837	0.003	0.170	99.92	98.31	1.001	1.017
Backup system	5.863	3.985	2.712	1.834	53.70	53.94	1.862	1.854
Superheater	5.660	7.890	0.543	0.340	90.41	97.08	1.106	1.030
WtE boiler	56.338	56.338	37.186	36.546	33.99	35.13	2.941	2.846
Steam cycle	23.650	27.342	10.690	10.828	59.84	58.31	1.715	1.656
Total	72.1464	83.3831	57.994	66.869	19.62	19.80	5.0979	5.0493

It is notable that the higher exergy loss occurs in the boiler. For both cases, the exergy loss in boiler accounts for 64% and 54% (for case 1 and case 27, respectively). This result is also confirmed by Almutairi et al. [43], who reported the highest exergy loss (60.9%) in the combustion chamber. Exergy destruction of this component is caused by irreversibilities connected with chemical reaction, internal energy exchange, heat transfer and the mixing process.

The contribution to the total exergy loss of steam cycle is around 16 and 17%. Also, it can be observed that exergy loss in the solar subsystem composed by heliostat, receiver and storage tanks, contributes significantly to the total exergy loss. The exergy efficiency of the solar subsystem, which includes the heliostat field, receiver and storage tanks, is around 25%, which therefore results to be the least efficient component of the plant. Similar results were obtained by Zhu et al. [20] which found the exergy efficiency of the solar subsystem constituted from solar tower and heliostat to be 26%. With the increase of a share of solar input, the exergy loss from solar subsystem becomes more significant, contributing with a share of 13.7% and 25.8% for case 1 and case 27, respectively. The cause of such an amount of exergy loss in the solar subsystem is that solar energy of high quality is transferred to the

fluid at a lower temperature. In addition, for case 1, the loss from solar subsystem is 2.7 times greater than the loss from the gas backup system, while for case 27, which is characterized by higher solar share, the ratio between the two losses is around 9.4. However, the exergy efficiency related to case 27 is higher than that for case 1. This is obviously caused by the fact that, for higher temperature and pressure values, the more useful product is generated.

Tables 4 and 5 present the comparison of the results of exergy analysis for the integrated solar system (Table 4) and gas integrated system (Table 5). By comparing the cases for the same solar part design parameters (SM and time of storage), it can be noticed that exergy efficiency increases with the increasing of steam parameters. As an example, for SM = 1.5 and t = 6 h and relative cases 1, 10 and 19, the resulting second law efficiency is 19.62%, 20.35% and 21.06%, respectively. A similar trend appears in other cases. Apparently, high values of the design steam parameters positively affect the net power output and the net efficiency of the steam cycle. In contrast, by comparing the results within cases of the same steam parameters, it can be noticed that the average exergy efficiency of the entire system is lower for higher shares of solar exergy input. This can be explained by the increasing contribution of sources with relatively low exergy efficiency. Moreover, such an effect seems to be more evident for higher values of steam parameters, thus the higher requirements of superheating and larger solar fields. It is also observed that the thermal storage size seems to have a minor influence on the final efficiency.

**Table 4.** Exergy analysis results for the cases with solar superheating.

Case No.	Steam Parameters bar/°C	Solar Multiple/Time of Storage -/h	Exergy Received			Exergy Loss MW/MW	Second Law Efficiency %
			MSW, MW	Natural Gas, MW	Solar, MW		
1	51.0/440	1.5/6	56.34	5.86	9.95	55.25	19.62
2		1.5/10	56.34	5.86	9.95	55.25	19.62
3		1.5/14	56.34	5.86	9.95	55.25	19.62
4		2.0/6	56.34	4.41	13.24	57.10	19.13
5		2.0/10	56.34	4.29	13.24	56.98	19.16
6		2.0/14	56.34	4.29	13.24	56.98	19.16
7		2.5/6	56.34	3.27	16.55	59.27	18.59
8		2.5/10	56.34	2.99	16.55	58.99	18.66
9		2.5/14	56.34	2.86	16.55	58.86	18.69
10	60.0/480	1.5/6	56.34	6.99	11.87	57.10	20.35
11		1.5/10	56.34	6.98	11.87	57.10	20.35
12		1.5/14	56.34	6.98	11.87	57.10	20.35
13		2.0/6	56.34	5.25	15.75	59.25	19.78
14		2.0/10	56.34	5.11	15.75	59.11	19.81
15		2.0/14	56.34	5.11	15.75	59.11	19.82
16		2.5/6	56.34	3.89	19.75	61.89	19.14
17		2.5/10	56.34	3.56	19.75	61.55	19.22
18		2.5/14	56.34	3.41	19.75	61.40	19.26
19	70.0/520	1.5/6	56.34	8.17	13.81	58.96	21.06
20		1.5/10	56.34	8.17	13.81	58.95	21.06
21		1.5/14	56.34	8.17	13.81	58.95	21.06
22		2.0/6	56.34	6.15	18.49	61.61	20.40
23		2.0/10	56.34	5.98	18.49	61.45	20.44
24		2.0/14	56.34	5.98	18.49	61.44	20.44
25		2.5/6	56.34	4.55	23.06	64.58	19.66
26		2.5/10	56.34	4.17	23.06	64.20	19.76
27		2.5/14	56.34	3.99	23.06	64.02	19.80

**Table 5.** Exergy analysis results for the cases with gas superheating.

Case No.	Steam Parameters bar/°C	Solar Multiple/Time of Storage -/h	Exergy Received			Exergy Loss MW/MW	Second Law Efficiency %
			MSW, MW	Natural Gas, MW	Solar, MW		
1*	51.0/440	-	56.34	10.57	-	52.30	21.8
2*	60.0/480	-	56.34	12.59	-	53.11	22.9
3*	70.0/520	-	56.34	14.73	-	53.98	24.0

Table 5 shows the results, regarding exergy analysis, for cases 1\*–3\*, which assume that superheating the steam is entirely performed by natural gas. Generally, such systems are characterized by higher exergy efficiency values concerning the ones of integrated solar schemes, when the same steam parameters are considered. For these systems, the required superheating demand is covered by the source of higher exergy efficiency.

The presented results of exergy analysis indicate that the more favorable system is the one supported by non-renewable energy. This can also be observed from Figure 6 which present the exergy costs for the systems considered.

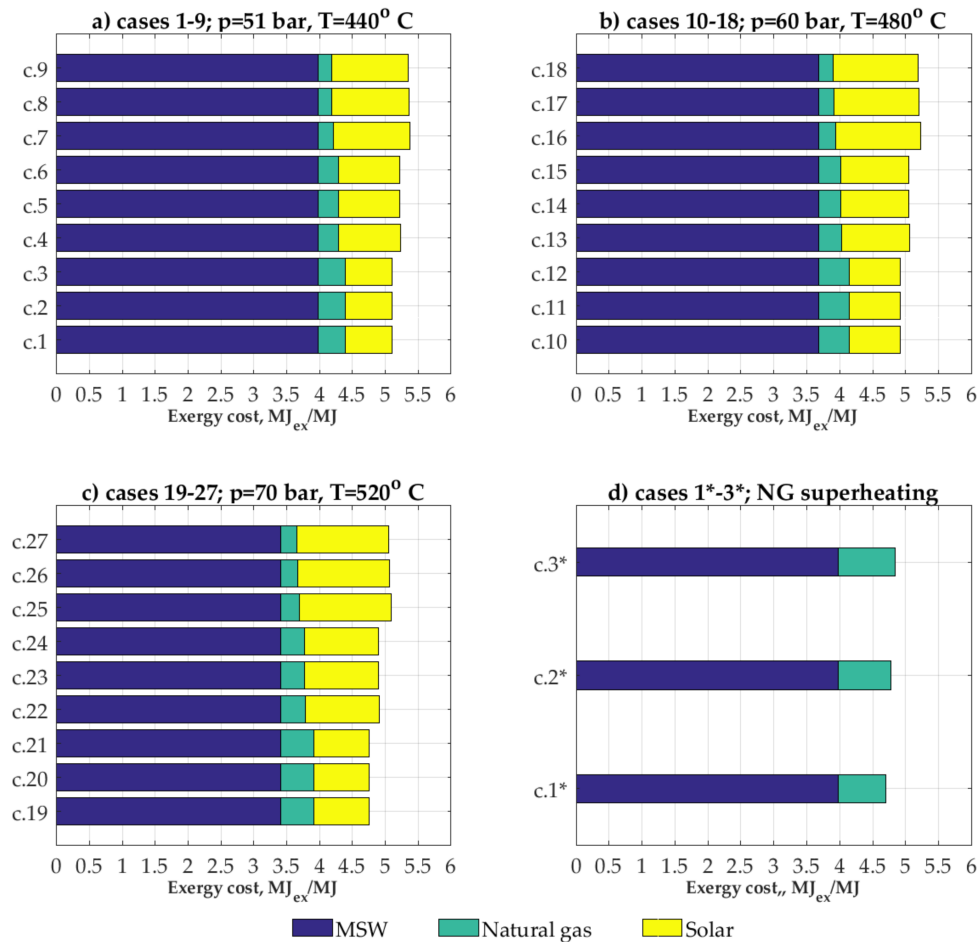


Figure 6. Exergy cost of the electricity for the analyzed cases (a–d).

For the solar integrated plant layouts, the exergy cost varies from 5.10 to 5.38  $\text{MJ}_{\text{ex}}/\text{MJ}$ , from 4.95 to 5.22  $\text{MJ}_{\text{ex}}/\text{MJ}$  and from 4.75 to 5.09  $\text{MJ}_{\text{ex}}/\text{MJ}$  for cases presented in subplots (a), (b), (c), respectively. The exergy cost of electricity produced in gas integrated schemes with the corresponding steam parameters and superheating demand, presented in subplot (d), are generally lower than for solar integrated cases, with values 4.15, 4.36 and 4.58  $\text{MJ}_{\text{ex}}/\text{MJ}$ . The relative increase of the values of exergy cost varies from 12% to 15% considering the average exergy cost value for the cases and it is more significant for the cases with higher superheating demand. Moreover, it can be also noticed that the exergy cost increase with the increase of a share of solar input and decreasing the gas input.

The exergy cost of the produced electricity only depends on the exergy efficiency of system components, not recognizing the origin of the driving exergy for particular components. This can lead to misleading conclusions indicating that non-renewable energy should be maximized. For this reason, the systems supplied by a mix of renewable and non-renewable energy sources should be analyzed in

extended form, taking into consideration the common balance boundary which is the level of natural resources. Such an assumption is included in the thermoecological cost analysis.

Figure 7 shows the results of the thermoecological cost analysis including the whole season of operation. Values of TEC of direct resources, input flows and emissions used in the analysis were calculated on the basis of the Ecoinvent 3.0 database and are presented in Table S2 of Supplementary File. Results depicted in Figure 7 are also presented in Table S3 of Supplementary File.

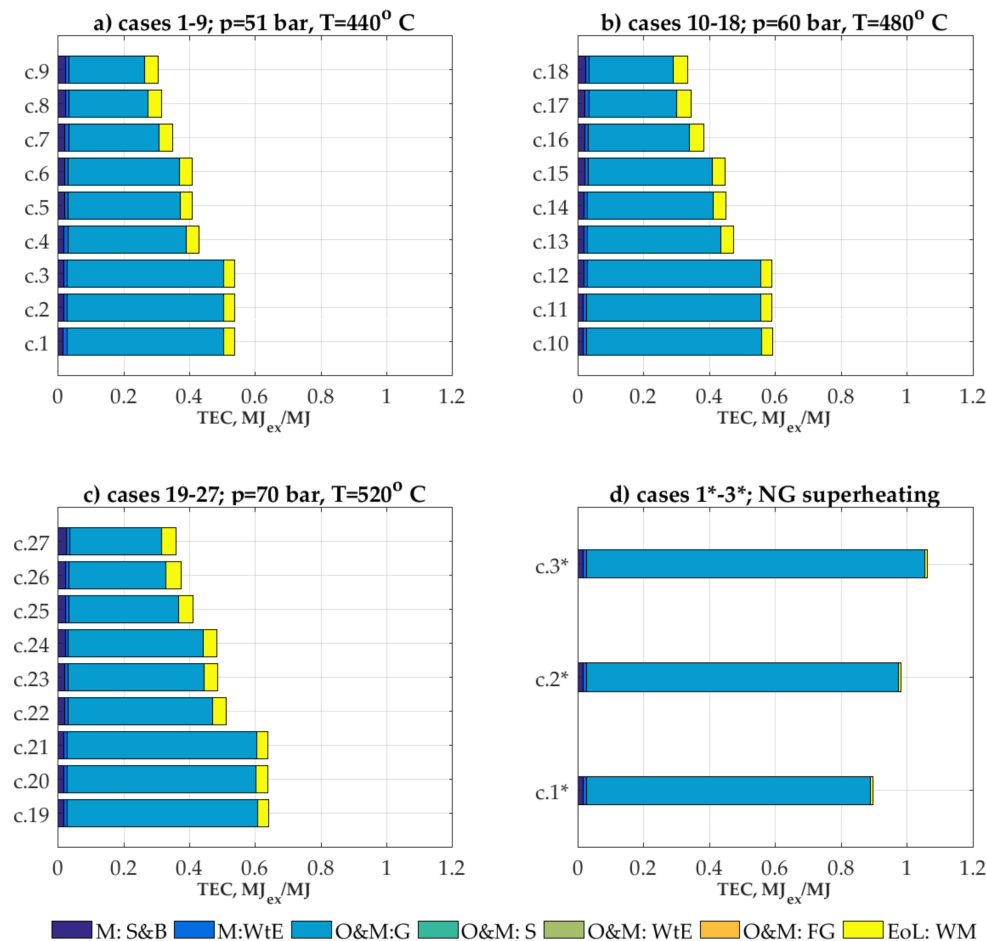


**Figure 7.** Thermoecological cost of the electricity for the analyzed cases (a–d) M:S&B—manufacturing stage: solar and gas backup cycle, M:WtE—manufacturing stage: WtE plant, O&M:G—operational stage: gas consumption, O&M:S—operational stage: solar field maintenance, O&M:WtE—operational stage: waste consumption; O&M:FG—operational stage: flue gas treatment; EoL:WM—end of life stage and waste management.

For the solar integrated plant layouts, the TEC varies from 0.26 to 0.50  $\text{MJ}_{\text{ex}}/\text{MJ}$ , from 0.29 to 0.56  $\text{MJ}_{\text{ex}}/\text{MJ}$  and from 0.31 to 0.61  $\text{MJ}_{\text{ex}}/\text{MJ}$  for cases presented in subplots a), b) and c) respectively. The result obtained for the gas integrated plant ranges between 0.87 and 1.04  $\text{MJ}_{\text{ex}}/\text{MJ}$ . The higher contributor to the TEC is the gas consumption (followed by the construction and end of life stage for the solar and gas backup subsystems). Thus, an opposite trend, with respect to the one for the exergy cost, is obtained. In addition, it can be noticed that the TEC increases for higher values of steam parameters since such a system requires a significant amount of input non-renewable exergy as well as larger solar fields. On the contrary, the TEC values decrease with the share of solar energy. It was shown that for all the cases employing solar energy, it was possible to obtain the product TEC below unity, which means that the exergy of resources used to generate the product is less than the exergy

value of that product. It can be concluded that, the TEC analysis leads to a proper evaluation of the system, showing the renewable resources efficiency and its ecological profitability.

In both, exergy cost and TEC analyses, the final result depended mainly on the superheating demand, and the contribution of renewable and non-renewable inputs. As a next step, a sensitivity analysis was performed in order to integrate the results and to indicate the critical variables. The sensitivity analysis was performed adopting the perturbation analysis developed by Heijungs et al. [44]. The variables were restricted to the temperature and pressure of steam facing the turbine as main parameters characterizing the superheating demand and the area of heliostats and thermal storage capacity as the factors affecting the contribution of renewable and non-renewable resources. The parameters were varied individually, (by increasing the value input parameter by 10 °C for temperature, 10 bar for pressure, 10% for area of collector and storage capacity) and as a consequence, the resulting variations in exergy cost and TEC were calculated. The sensitivity of the results is expressed by sensitivity ratio (SR) that is defined as follows:

$$SR = \frac{\frac{\Delta result}{initial\ result}}{\frac{\Delta parameter}{initial\ parameter}} \quad (20)$$

An absolute value of the SR higher than 0.8 indicates that the results are strongly affected by the input variations, while when value of SR is lower than 0.2 the input variations are considered as not significant [44]. Figures 8 and 9 show the results of the conducted sensitivity analysis.

In general, it can be noticed considerable influence of variations of temperature, pressure and area of heliostats on the final value of exergy cost. Absolute values of Sensitivity Ratios for exergy cost obtained by varying temperature, pressure and area of heliostat were in the range from 0.30–0.35; 0.20–0.22; 0.56–0.67, respectively. It was observed that by increasing both the temperature, and the pressure of superheated steam, it is possible to reduce the value of exergy cost (negative value of SR). The SR value for temperature slightly increases for cases with higher superheating demand. On the contrary, the importance of steam pressure decreases with the increasing superheating demand. This trend is also observed for the gas superheating cases, as depicted in subplot d).

As far as solar design parameters are considered, by increasing the area of collector the exergy cost will increase (SR positive). Moreover, the area of collector has the major influence on the exergy cost for all the solar integrated cases. The results are not affected by the variations in thermal storage capacity. However, for all the parameters analyzed the SR value does not exceed 0.8.



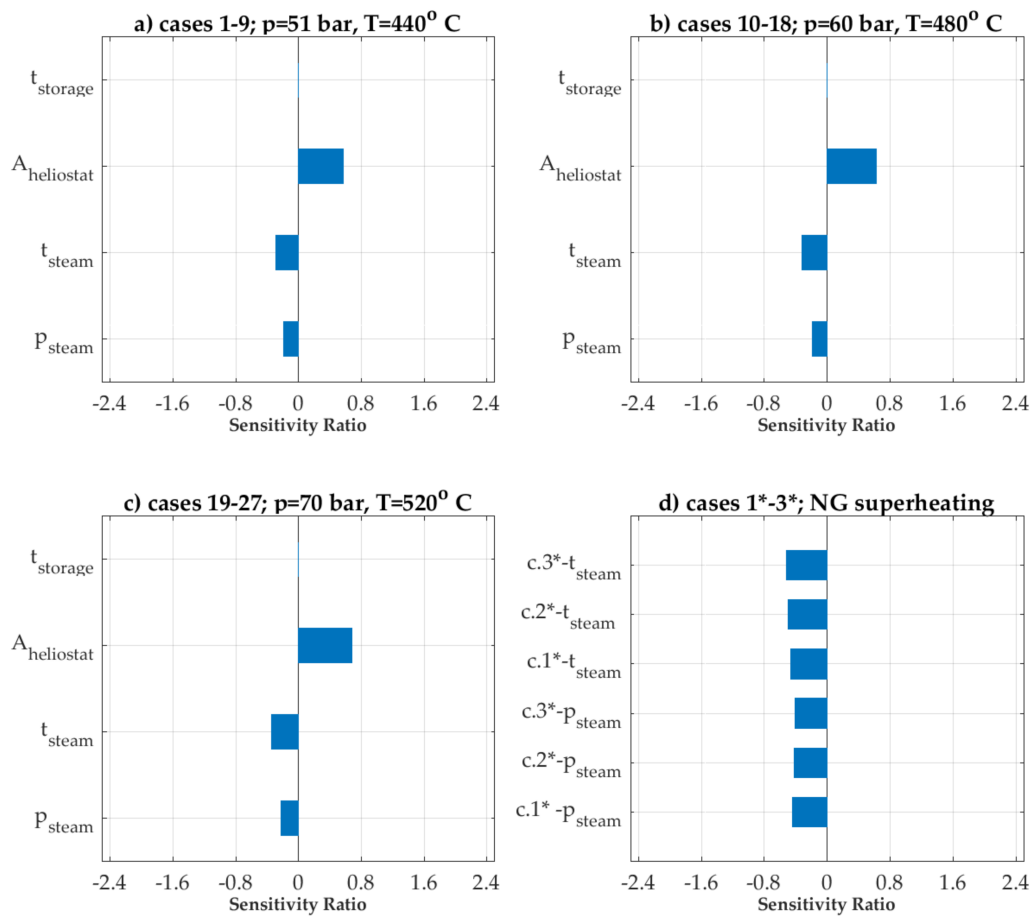


Figure 8. Sensitivity Ratio of exergy cost for the analyzed cases (a–d).

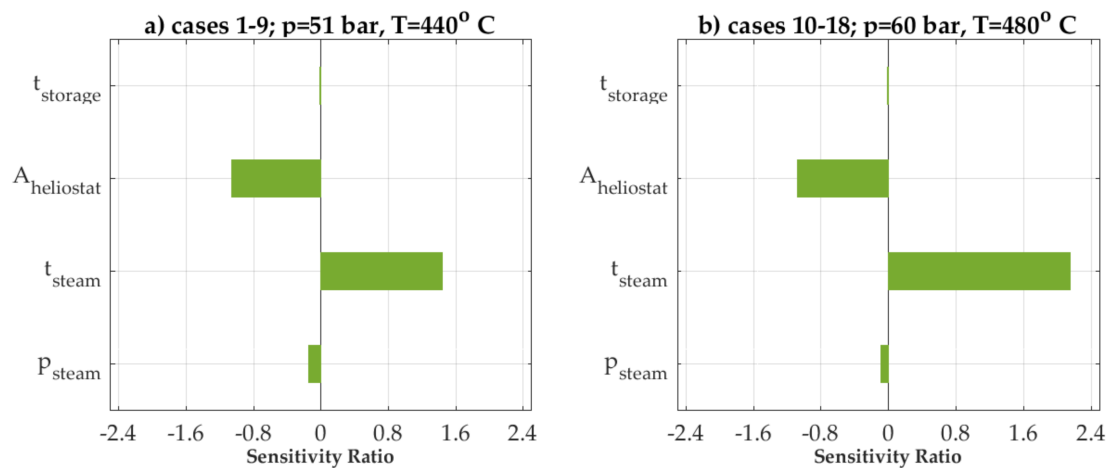


Figure 9. Cont.

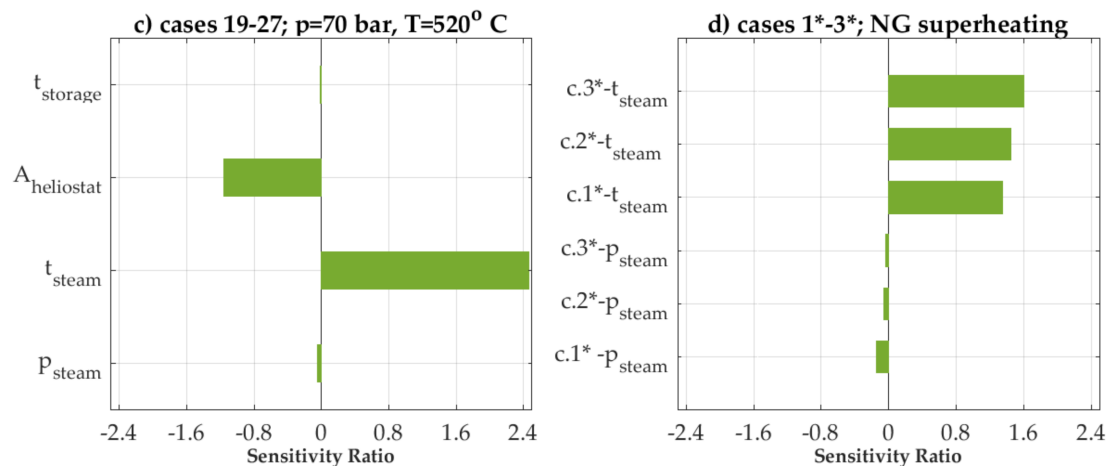


Figure 9. Sensitivity Ratio of thermoecological cost for the analyzed cases (a–d).

More evident result was obtained for the SR of thermoecological cost. For this indicator, changes of two variables i.e., steam temperature and area of heliostat resulted in significant variation of the final result. In both cases of variables, SR exceeded value of 0.8. The highest value of SR was observed for steam temperature. Increasing of temperature, the corresponding superheating demand and gas consumption increase deteriorating the final TEC. On the contrary, by increasing the area of collector, thus the solar contribution, it is possible to reduce notably the exergoecological impact of electricity. Similarly to exergy cost, minor effect of storage capacity variations was observed for TEC (SR below 0.01). Moreover, the changes of steam pressure resulting in SR from 0.04 to 0.14 also seem to not affect the final result of TEC.

#### 4. Conclusions

In this study, a comprehensive exergy analysis of the integrated solar—WtE plant was conducted. The performance assessment was carried out by considering exergy and thermoecological cost. It was shown that the highest exergy destruction occurs in the boiler. However, the solar subsystem is the least efficient component of the plant. The exergy cost is lower for the plant schemes characterized by higher values of steam parameters. However, it was found that the additional solar energy input to the system negatively affects the exergy efficiency and, therefore, influences the exergy cost of electricity with higher share of solar exergy input. Moreover, the exergy cost of electricity for gas-integrated plants is lower than that related to solar integrated schemes, when the same values for the steam parameters are considered.

An opposite result was obtained for thermoecological cost. As the highest contributor to the TEC was gas consumption, the thermoecological cost resulted greater for cases characterized by higher shares of natural gas input, thus the lower solar input. The parameters affecting significantly the final results were found to be temperature and area of heliostats.

The results of the study demonstrate the importance of the origin of the energy carriers supplied to the WtE plant. Output of exergy cost analysis is crucial when minimizing internal plant irreversibilities, but it suggests to minimize the solar energy utilization in the system. However, it was presented that it is possible to obtain the product TEC below unity in the solar integrated cases, which means that the exergy of resources used to generate the product is less than the exergy value of that product.

In general, it can be therefore concluded that the TEC analysis leads to a correct evaluation of a multi-energy system, by showing the renewable resources efficiency and their ecological profitability.

**Supplementary Materials:** The following are available online at <http://www.mdpi.com/1996-1073/11/4/773/s1>, Table S1 Performance outputs for analyzed WtE + CSP cases, Table S2: Thermoecological cost data for inputs used in analysis, Table S3: Thermoecological cost of the electricity for the analyzed cases, M: S& B—manufacturing

stage: solar and gas backup cycle, M: WtE—manufacturing stage: WtE plant, O&M: G—operational stage: gas consumption, O&M: S—operational stage:—solar field maintenance, O&M: WtE—operational stage: waste consumption; O&M: FG—operational stage: flue gas treatment; EoL: WM—end of life stage and waste management.

**Author Contributions:** In this article, Barbara Mendecka was the principal investigator. Lidia Lombardi proposed the idea and designed the different phases of the research. Paweł Gładysz was involved in the development of the thermodynamic model. Wojciech Stanek supervised the work in terms of exergy analysis.

**Conflicts of Interest:** The authors declare no conflict of interest.

## References

1. European Parliament and Council. Directive 2008/98/EC of the European Parliament and of the Council of 19 November 2008 on waste and repealing certain directives. *Off. J. Eur. Union* **2008**, 3–30. Available online: <http://www.reach-compliance.eu/english/legislation/docs/launchers/waste/launch-2008-98-EC.html> (accessed on 11 March 2018).
2. European Commission. Communication from the Commission to the European Parliament, the Council, the European Economic and Social Committee and the Committee of the Regions: The Role of Waste-to-Energy in the Circular Economy COM/2017/0034. 2017. Available online: <http://ec.europa.eu/environment/waste/waste-to-energy.pdf> (accessed on 11 March 2018).
3. Zhang, D.; Huang, G.; Xu, Y.; Gong, Q. Waste-to-energy in China: Key challenges and opportunities. *Energies* **2015**, *8*, 14182–14196. [[CrossRef](#)]
4. Reimann, D.O. *CEWEP Energy Report III (Status 2007–2010)*; Confederation of European Waste-to-Energy Plants: Wurzburg, Germany, 2013; pp. 1–35.
5. Palstra, S.W.L.; Meijer, H.A.J. Carbon-14 based determination of the biogenic fraction of industrial CO<sub>2</sub> emissions—Application and validation. *Bioresour. Technol.* **2010**. [[CrossRef](#)] [[PubMed](#)]
6. Cardoso, J.; Silva, V.; Eusébio, D.; Brito, P. Hydrodynamic modelling of municipal solid waste residues in a pilot scale fluidized bed reactor. *Energies* **2017**, *10*, 1773. [[CrossRef](#)]
7. Eriksson, O.; Finnveden, G. Energy Recovery from Waste Incineration—The Importance of Technology Data and System Boundaries on CO<sub>2</sub> Emissions. *Energies* **2017**, *10*, 539. [[CrossRef](#)]
8. Rocco, M.V.; Di Lucchio, A.; Colombo, E. Exergy Life Cycle Assessment of electricity production from Waste-to-Energy technology: A Hybrid Input-Output approach. *Appl. Energy* **2017**, *194*, 832–844. [[CrossRef](#)]
9. Lee, S.-H.; Themelis, N.J.; Castaldi, M.J. High-Temperature Corrosion in Waste-to-Energy Boilers. *J. Therm. Spray Technol.* **2007**, *16*, 104–110. [[CrossRef](#)]
10. Persson, K.; Broström, M.; Carlsson, J.; Nordin, A.; Backman, R. High temperature corrosion in a 65 MW waste to energy plant. *Fuel Process. Technol.* **2007**, *88*, 1178–1182. [[CrossRef](#)]
11. Martin, J.J.E.; Koralewska, R.; Wohlleben, A. Advanced solutions in combustion-based WtE technologies. *Waste Manag.* **2015**, *37*, 147–156. [[CrossRef](#)] [[PubMed](#)]
12. Lombardi, L.; Carnevale, E.; Corti, A. A review of technologies and performances of thermal treatment systems for energy recovery from waste. *Waste Manag.* **2015**, *37*, 26–44. [[CrossRef](#)] [[PubMed](#)]
13. Consonni, S.; Silva, P. Off-design performance of integrated waste-to-energy, combined cycle plants. *Appl. Therm. Eng.* **2007**, *27*, 712–721. [[CrossRef](#)]
14. Cucchiella, F.; D'Adamo, I.; Gastaldi, M. The Economic Feasibility of Residential Energy Storage Combined with PV Panels: The Role of Subsidies in Italy. *Energies* **2017**, *10*, 1434. [[CrossRef](#)]
15. Lombardi, L.; Mendecka, B.; Carnevale, E. WtE efficiency improvements: Integration with solar thermal energy. In Proceedings of the 5th International Conference on Sustainable Solid Waste Management, Athens, Greece, 21–24 June 2017.
16. Wang, L.; Yang, Y.; Morosuk, T.; Tsatsaronis, G. Advanced Thermodynamic Analysis and Evaluation of a Supercritical Power Plant. *Energies* **2012**, *5*, 1850–1863. [[CrossRef](#)]
17. Cozzolino, R. Thermodynamic Performance Assessment of a Novel Micro-CCHP System Based on a Low Temperature PEMFC Power Unit and a Half-Effect Li/Br Absorption Chiller. *Energies* **2018**, *11*, 315. [[CrossRef](#)]
18. Eboh, F.; Ahlström, P.; Richards, T. Exergy Analysis of Solid Fuel-Fired Heat and Power Plants: A Review. *Energies* **2017**, *10*, 165. [[CrossRef](#)]

19. Toro, C.; Rocco, M.; Colombo, E. Exergy and Thermo-economic Analyses of Central Receiver Concentrated Solar Plants Using Air as Heat Transfer Fluid. *Energies* **2016**, *9*, 885. [[CrossRef](#)]
20. Zhu, Y.; Zhai, R.; Peng, H.; Yang, Y. Exergy destruction analysis of solar tower aided coal-fired power generation system using exergy and advanced exergetic methods. *Appl. Therm. Eng.* **2016**, *108*, 339–346. [[CrossRef](#)]
21. Peng, S.; Wang, Z.; Hong, H.; Xu, D.; Jin, H. Exergy evaluation of a typical 330 MW solar-hybrid coal-fired power plant in China. *Energy Convers. Manag.* **2014**, *85*, 848–855. [[CrossRef](#)]
22. Manente, G.; Rech, S.; Lazzaretto, A. Optimum choice and placement of concentrating solar power technologies in integrated solar combined cycle systems. *Renew Energy* **2016**, *96*, 172–189. [[CrossRef](#)]
23. Baghernejad, A.; Yaghoubi, M. Exergy analysis of an integrated solar combined cycle system. *Renew. Energy* **2010**, *35*, 2157–2164. [[CrossRef](#)]
24. Mathkor, R.; Agnew, B.; Al-Weshahi, M.; Latrsh, F. Exergetic Analysis of an Integrated Tri-Generation Organic Rankine Cycle. *Energies* **2015**, *8*, 8835–8856. [[CrossRef](#)]
25. Bellos, E.; Tzivanidis, C. Optimization of a Solar-Driven Trigenation System with Nanofluid-Based Parabolic Trough Collectors. *Energies* **2017**, *10*, 848. [[CrossRef](#)]
26. Calise, F.; Capuano, D.; Vanoli, L. Dynamic Simulation and Exergo-Economic Optimization of a Hybrid Solar–Geothermal Cogeneration Plant. *Energies* **2015**, *8*, 2606–2646. [[CrossRef](#)]
27. Calise, F.; d’Accadia, M.; Piacentino, A.; Vicidomini, M. Thermo-economic Optimization of a Renewable Polygeneration System Serving a Small Isolated Community. *Energies* **2015**, *8*, 995–1024. [[CrossRef](#)]
28. Usón, S.; Kostowski, W.J.; Stanek, W.; Gazda, W. Thermoecological cost of electricity, heat and cold generated in a trigeneration module fuelled with selected fossil and renewable fuels. *Energy* **2015**, *92*, 308–319. [[CrossRef](#)]
29. Szargut, J. *Exergy Method: Technical and Ecological Applications*; WIT Press: Boston, MA, USA, 2005.
30. Szargut, J.; Zibik, A.; Stanek, W. Depletion of the non-renewable natural exergy resources as a measure of the ecological cost. *Energy Convers. Manag.* **2002**, *43*, 1149–1163. [[CrossRef](#)]
31. Lombardi, L.; Mendecka, B.; Carnevale, E. Comparative life cycle assessment of alternative strategies for energy recovery from used cooking oil. *J. Environ. Manag.* **2017**. [[CrossRef](#)] [[PubMed](#)]
32. Mendecka, B.; Lombardi, L.; Koziol, J. Probabilistic multi-criteria analysis for evaluation of biodiesel production technologies from used cooking oil. *Renew. Energy* **2017**. [[CrossRef](#)]
33. Lombardi, L.; Mendecka, B.; Carnevale, E.; Stanek, W. Environmental impacts of electricity production of micro wind turbines with vertical axis. *Renew. Energy* **2017**. [[CrossRef](#)]
34. Czarnowska, L.; Stanek, W.; Pikoń, K.; Nadziakiewicz, J. Environmental quality evaluation of hard coal using LCA and exergo-ecological cost methodology. *Chem. Eng. Trans.* **2014**, *42*, 139–144. [[CrossRef](#)]
35. Stanek, W.; Gazda, W.; Kostowski, W. Thermo-ecological assessment of CCHP (combined cold-heat-and-power) plant supported with renewable energy. *Energy* **2015**, *92*, 279–289. [[CrossRef](#)]
36. Soares, T.; Silva, M.; Sousa, T.; Morais, H.; Vale, Z. Energy and Reserve under Distributed Energy Resources Management—Day-Ahead, Hour-Ahead and Real-Time. *Energies* **2017**, *10*, 1778. [[CrossRef](#)]
37. Morris, D.R.; Szargut, J. Standard chemical exergy of some elements and compounds on the planet earth. *Energy* **1986**, *11*, 733–755. [[CrossRef](#)]
38. Omendra, S.C.K.; Singh, K. Estimation of chemical exergy of solid, liquid and gaseous fuels used in thermal power plants. *J. Therm. Anal. Calorim.* **2013**, *115*, 903–908. [[CrossRef](#)]
39. Petela, R. Exergy of undiluted thermal radiation. *Sol. Energy* **2003**, *74*, 469–488. [[CrossRef](#)]
40. Stanek, W.; Gazda, W. Exergo-ecological evaluation of adsorption chiller system. *Energy* **2014**, *76*, 42–48. [[CrossRef](#)]
41. Saidur, R.; BoroumandJazi, G.; Mekhlif, S.; Jameel, M. Exergy analysis of solar energy applications. *Renew. Sustain. Energy Rev.* **2012**, *16*, 350–356. [[CrossRef](#)]
42. Stanek, W. (Ed.) *Thermodynamics for Sustainable Management of Natural Resources*; Springer International Publishing: Cham, Switzerland, 2017.

43. Almutairi, A.; Pilidis, P.; Al-Mutawa, N. Energetic and Exergetic Analysis of Combined Cycle Power Plant: Part-1 Operation and Performance. *Energies* **2015**, *8*, 14118–14135. [[CrossRef](#)]
44. Heijungs, R.; Kleijn, R. Numerical approaches towards life cycle interpretation five examples. *Int. J. Life Cycle Assess.* **2001**, *6*, 141–148. [[CrossRef](#)]



© 2018 by the authors. Licensee MDPI, Basel, Switzerland. This article is an open access article distributed under the terms and conditions of the Creative Commons Attribution (CC BY) license (<http://creativecommons.org/licenses/by/4.0/>).